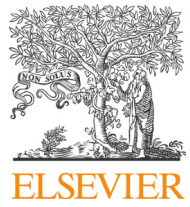

Procedia Manufacturing

Volume 1, 2015, Pages 607–618

43rd Proceedings of the North American Manufacturing Research Institution of SME http://www.sme.org/namrc

Ultra-Precision Machining Process Dynamics and Surface Quality Monitoring

Changqing Cheng[1], Zimo Wang[2], Wayne Hung[2], Satish T.S. Bukkapatnam[2,*] and Ranga Komanduri[3]

[1]*Industrial and Management Systems Engineering, University of South Florida, Tampa, FL, USA,*
[2]*Department of Industrial and Systems Engineering, Texas A&M University, College Station, TX,*
[3]*Mechanical and Aerospace Engineering, Oklahoma State University, Stillwater, OK*
[*]satish@tamu.edu

Abstract

Surface finish deterioration in the ultra-precision machining (UPM) process is often attributed to dynamic instabilities. Models and approaches to predict UPM process instabilities are in their infancy. In the present work, UPM dynamics and its relationship to surface characteristics are studied using a combined analytical modeling and experimental effort. A one degree-of-freedom delay differential equation model that incorporates the joint effects of shear and ploughing taking place at sub-micrometer scale machining is investigated to capture the source of vibrations in UPM dynamics. A temporal finite element method (TFEM) was used to simplify the model to facilitate validation studies. The model was verified using an experimental UPM setup integrated with three accelerometers, a 3-axis dynamometer and an acoustic emission (AE) sensor. The setup was employed for face turning of 6061 aluminum workpiece using a single point polycrystalline diamond tool at different cutting conditions. The surface characteristics were measured offline using MicroXam®, a confocal optical microscope. Experimental investigations suggest that the model predictions of stability characteristics match 70% of the experimental observations. Additionally, even under stable UPM process conditions determined based on the analytical model, surface roughness of UPM machined workpieces varied significantly due to uncertainties associated with complex chip formation process, thermal effects and other uncontrollable factors. A sensor-based approach based on a nonparametric Gaussian process model was used to estimate surface roughness (Ra) using statistical and nonlinear features from force and vibration signals recorded at UPM process. Over 80% of the Ra estimations under test condition were consistent with the experiment measurements. Hence, by combining the physical and statistical models, we can choose suitable "stable" process conditions to yield surface finish Ra in 10-50 nm range, and estimate the surface roughness changes in real-time.

Keywords: Dynamics stability model, Surface integrity, Ultra-precision machining

Satish T.S. Bukkapatnam, Department of Industrial and Systems Engineering, Texas A&M University, College Station, TX, 77840, E-mail:satish@tamu.edu

Peer-review under responsibility of the NAMRI Scientific Committee
doi:10.1016/j.promfg.2015.09.044

1 Introduction

Industry relies on ultra-precision machining (UPM) to realize surface roughness (Ra) in the range of 1-100nm for applications such as telecommunications, defense, and biomedical product components (Dornfeld et al., 2006). For example, precision aluminum disks are widely used in the manufacturing of optical components in lasers, hard drives and memory discs in computer industry and rotating mirrors in copying machines (Ikawa et al., 1991). In contrast to conventional machining process, UPM involves a fine depth of cut, usually in the range of tens of nanometers to a few micrometers (Komanduri et al., 2000), and requires no subsequent post-machining processes (Lee et al., 1999). Surface finish assurance is critical to ensure many functional properties of the machined components (Patrikar, 2004, Ikawa et al., 1991).

Surface finish in UPM is known to depend heavily on the process dynamics; unstable cutting is considered as one of the chief detriments to surface quality assurance (Altintas and Weck, 2004). While proper machine design, such as increased stiffness and damping of the machine tool structure, can broaden the range of stable operating conditions, the inherent geometry of the tool and workpiece, and more importantly, the change of dynamic regimes can sometimes severely limit the range of stable cutting (Altintas et al., 2008). Surface quality issues have not been completely addressed in UPM due to the complex process dynamics.

Process dynamics models for conventional machining are not adequate to characterize the dynamics and predict instability in UPM. In UPM, the tool edge radius is comparable to the chip load, and is at the same order of magnitude with the grain size of the workpiece material. Consequentially, the effective rake angle tends to be highly negative. This gives rise to distinctly different chip-formation and machined surface generation mechanisms as well as magnitude of cutting and thrust forces and their ratios (Liu et al., 2004). Analytical, mostly frequency-domain models (Altintas and Weck, 2004, Jin and Altintas, 2013), have been employed to explore stability in conventional machining and, more recently, micro milling process. Suitable transfer functions are developed to represent the relationship between the force exerted on the tool and the corresponding displacement. Time domain models (Ahmadi and Ismail, 2010) have also been investigated to capture the effects of the kinematics of the metal cutting process, tool geometry and regenerative waviness. But the earlier models only considered the nonlinearity of structural stiffness or damping (Chae et al., 2006) and/or employed simple nonlinear expressions for forces generated during machining. For instance, Stepan et al. (Stepan et al., 2004) investigated high-speed milling process using a delay differential equation (DDE) model that uses a point cutting force of the form $F_x \propto h^{3/4}$, where h is the uncut chip thickness. The nonlinear relationship between the distributed cutting force and uncut chip thickness, as well as other edge radius effects which are pronounced in UPM dynamics, have not received much attention. A time-domain model that can capture the intrinsic relationship between dynamic chip formation process and system response is therefore needed to characterize and predict stability in UPM.

In this paper, we developed a physical model to explain the vibration and stability characteristics observed during UPM process experiments. The physical model for UPM process dynamics utilizes a nonlinear DDE with a spatially distributed force expression to describe the tool vibration in the feed direction, and thence characterize various stability regimes. Additionally, UPM is a highly nonlinear and nonstationary process, and the change of process dynamics can dramatically affect the surface characteristics (Rao et al., 2014). Experimental studies indicate that surface morphology in UPM can display sudden and almost abrupt variations (Rao et al., 2014), and surface anomaly development cannot be predicted even in a well-designed process. This paper also reports the fusion of the physical model with a sensor-based data-driven model to predict surface roughness variation. A multi-sensor (force signal and vibration signal) fusion technique was employed to capture the complex machining process, which may be difficult to explain using physical (dynamic) models. Features extracted from the signals were employed to predict surface roughness (Ra) variation. Experimental investigations

suggest that the physical model can identify the stability characteristics at different process parameter combinations with an accuracy of 70%, and a Gaussian process regression model estimate the surface roughness (Ra) from the measured vibration characteristics accurately (R^2~80%) relative to the experiment measurements. The remainder of this paper is organized as follows: Section 2 presents the research methodology; Section 3 contains the result from the physical and data-driven models; Conclusions are presented in Section 4.

2 Research Methodology

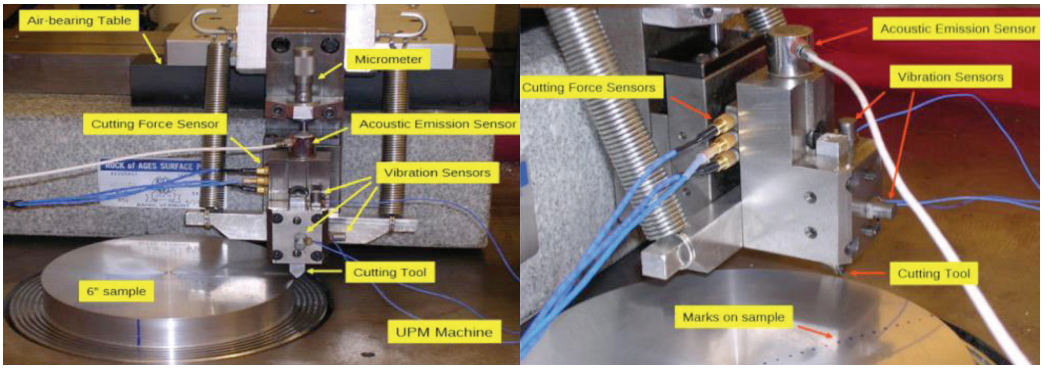

Figure 1: UPM experiment setup equipped with multiple sensors

The UPM setup for our experiments is shown in Figure 1 (Rao et al., 2014). It was designed for facing flat surfaces to achieve Ra in the range of 5-100 nm. The UPM machine is equipped with an aerostatic spindle bearing (model Block-Head® 4R) and air-slide tool carriage produced by Professional Instruments Inc. The whole setup rests on a 2 metric ton granite base for added stability. We used a polycrystalline diamond (PCD) cutting tool with 60 µm nose radius and Φ8cm ×3cm cylindrical 6061 aluminum discs as workpiece. Three Kistler 8728A500 vibration sensors were mounted along three orthogonal directions on the tool holder near the PCD cutting insert to measure vibration signals, and a Kistler 3-axis dynamometer was mounted on the underside of tool holder to measure force signals. Additionally, an acoustic emission (AE) sensor (R80) from Physical Acoustics was mounted on the top of tool holder. Sampling rates of 10 kHz were chosen for vibration and force signals, 1 MHz for acoustic emission signals.

At each process parameter setting (feed rate: 1.5, 3, 6 mm/min; depth of cut: 5, 10, 20, 25 µm; spindle speed: 500, 1000, 2000 rpm), the facing operation was performed on a separate workpiece with the tool moving from the periphery towards the center. It may be noted that the values of the feed and the depth of cut are on the higher side compared to most industrial UPM processes. However the process parameter combination was determined keeping with the repeatability and measurement limitations, as well as the need to explore dynamic regimes possible in the process. The workpiece surface was divided into 16 zones, each forming 4.5 mm wide ring within which the variation of the cutting speed and process characteristics such as chip morphology, was minimal. At the end of a facing operation, the surface roughness (Ra) at each marked zone was measured using MicroXAM®, a non-contact confocal optical microscope capable of estimating surface profiles to sub-nanometer accuracies. This UPM setup was able to achieve a mirror-like surface finish with Ra~20 nm (shown in Figure 2 (a) and (b)). However, sudden anomalous changes in surface characteristic (Figure 2 (c)) can occur even during stable cutting (e.g. sub surface scratches in Figure 2 (d)) due to uncertainties associated with material and microstructure inhomogeneities, environmental factors, etc. Our

sensor-based modeling approach can predict the onset of unstable machining and estimate the surface roughness in real-time.

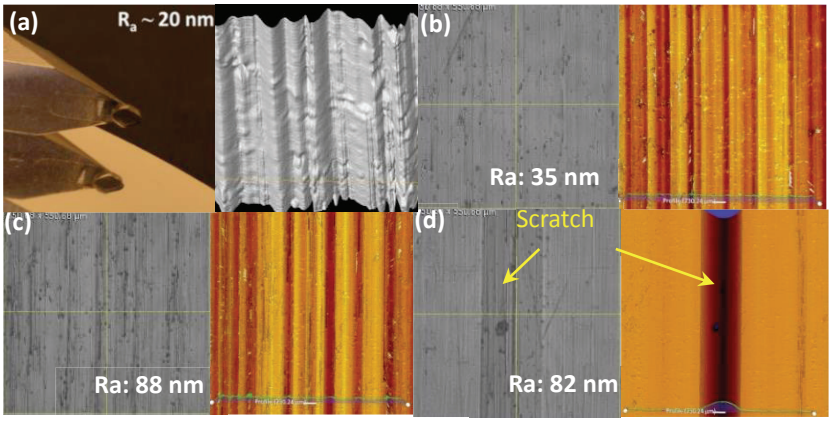

Figure 2: Image of surface finish under microscope (a) Surface with Ra~20 nm, (b) smooth surface (Ra around 35 nm), (c) surface with finish variation (Ra around 80 nm), and (d) surface with scratch

2.1 UPM process dynamics model

As opposed to conventional machining, tool edge in UPM cannot be assumed to be perfectly sharp; the effect of the edge radius R becomes prominent, and the effective rake angle becomes negative and progressively varies along the tool edge, as summarized in Figure 3(Liu et al., 2001). A stagnant point (A), is known to exist below which the material is subject only to elastic-plastic deformation or ploughing (Venkatachalam and Liang, 2006). Ploughing effect has been widely studied in machining process. However, most of the research work treated the ploughing and shearing as mutually exclusive phenomena (Venkatachalam and Liang, 2006). Son *et al.* (Son et al., 2005) proposed that since the ploughing action is significant at very small depths of cut, the coefficient of friction can no longer be assumed to be constant (Son et al., 2005). Most time-domain models represent the interaction between the cutting process and the machine tool-workpiece structure as a linear differential equations with time delay; the round edge or ploughing effect and nonlinearity arising from transcendental relationship connecting the friction phenomena to chip load are largely ignored (Bayly et al., 2003).

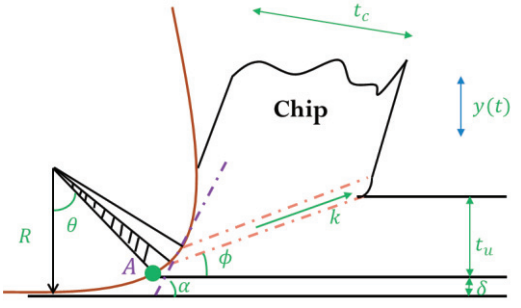

Figure 3: Schematic diagram of UPM process

We employed a single degree-of-freedom (dof) DDE model of the form $\ddot{y}(t) + 2\zeta\omega_n\dot{y}(t) + \omega_n^2 y(t) = -F_t/m$, to describe the relative vibration $y(t)$ between the cutting tool and the workpiece

in the feed direction in the UPM process. It was suggested from our recent work that vibrations in the feed direction contribute most to surface roughness variations in UPM (Rao et al., 2014). Here, m is the tool mass, ζ is the damping ratio, ω_n is the natural frequency, and F_t is the thrust force term that considers effects of the progressively varying (and mostly negative) rake angle, ploughing , as well as overlapped cutting in UPM.

As shown in Figure 3, δ represents the indentation depth, also known as the minimum cutting thickness. This can be estimated as $\delta = R\left[1 - cos(\frac{\pi}{4} - \frac{\beta}{2})\right]$ (Son et al., 2005), where β is the friction angle. The friction coefficient between diamond and metal is in the range of 0.05-0.5 according to test environment (De Barros et al., 2001). The uncut chip thickness is given by $t_u = f_0 - y(t) + y(t-T) - \delta = f_t - \delta$ where f_0 the nominal feed rate, f_t the actual feed at time t, T is the time delay, or the revolution period (to capture the overlapped cutting). Based on Waldorf *et al.* (Waldorf et al., 1999) , we expressed the dynamic shear angle as

$$\phi = \tan^{-1}\frac{f_t - \delta}{R\tan(\frac{\pi}{4}+\frac{\alpha}{2}) - \sqrt{2R\delta - \delta^2} + \frac{r_c(f_t-\delta)}{\cos\alpha} - f_t\tan\alpha} \quad (1)$$

We used the actual feed $f_t = f_0 - y(t) + y(t-T)$ instead of nominal feed f_0 used in a previous study (Waldorf et al., 1999). The chip thickness ratio r_c is treated as constant in the dynamic model since the variation of r_c due to vibrations can be neglected. But the chip load may be time-varying and is modeled as a function of $f(t)$. The effective take angle α is considered as a function of tool radius R and actual feed f_t, i.e., $\sin\alpha = \frac{f_t}{R} - 1$ (Venkatachalam and Liang, 2006).

According to (Son et al., 2005), a distributed force model is more appropriate for UPM. The resultant thrust force due to the shearing effect can be expressed as $F_\emptyset = \int_{\theta_1}^{\theta_2} \frac{kwR\,cos(\beta+\theta)sin\theta}{sin\,\phi\,sin(\phi+\beta+\theta)} d\theta$, where $\theta_1 = cos^{-1}\,(1 - \frac{\delta}{R})$ and $\theta_2 = cos^{-1}(1 - \frac{f_t}{R})$, k is the shear flow stress (for 6061 aluminum, $k = 226.5\text{N/mm}^2$) (Waldorf et al., 1999), and w represents the chip width in the face turning operation. The ploughing force can be given as $F_p = \int_0^{\theta_1} pwR(sin\,\theta + \mu_p\,cos\,\theta)\,d\theta$, where p is the stress along the tool edge below the stagnant point A, and μ_p is the friction coefficient. The ploughing force is accumulated along the tool below A. Therefore, the dynamic model for UPM process is expressed as

$$\ddot{y}(t) + 2\zeta\omega_n\dot{y}(t) + \omega_n^2 y(t) = -[F_\emptyset + F_p\,]/m \quad (2)$$

The solution of Eq. (2) represents the stability of the UPM process. However, it is non-trivial to solve Eq. (2) due to the integral form with time delay, and no closed-form solutions are available for such DDEs. Therefore, we first implemented 1-dof DDE in MATLAB Simulink module. This direct simulation is cumbersome, and requires extra efforts to investigate the stability at different parameter combinations. As a numerical method, TFEM has been recently studied in literature to approximate the solution and examine the stability of conventional machining process (Peters and Idzapanah, 1988, Bayly et al., 2003) with linear force models. To adapt TFEM to explore UPM process dynamics, we linearized the force term on the right hand side of Eq. (2), and obtained the following

$$\ddot{y}(t) + 2\zeta\omega_n\dot{y}(t) + \omega_n^2 y(t) = -\left\{\left(1 + \frac{\pi}{2}\right)C_1 - 2C_2 - 1\right\}\left(f_0 - y(t) + y(t-T)\right) \quad (3)$$

Here, $C_1 = \cot\phi$ and $C_2 = \phi/\tan\phi$. The time duration of each revolution of the workpiece is divided into multiple elements, and the displacement of the cutting tool at the j^{th} time element in the n^{th} revolution can be approximated as a linear combination of interpolated polynomials as $y(t) = \sum_{i=1}^{4} a_{ji}^n S_i(\sigma)$, where σ is the local time within the j^{th} element. The trial functions $S_i(\sigma)$ are the cubic Hermite polynomials. In the j^{th} element, those trial functions are given as (Bayly et al., 2003)

$$S_1(\sigma) = 1 - 3\left(\frac{\sigma}{t_j}\right)^2 + 2\left(\frac{\sigma}{t_j}\right)^3 \quad S_2(\sigma) = t_j\left[\frac{\sigma}{t_j} - 2\left(\frac{\sigma}{t_j}\right)^2 + \left(\frac{\sigma}{t_j}\right)^3\right]$$
$$S_3(\sigma) = 3\left(\frac{\sigma}{t_j}\right)^2 - 2\left(\frac{\sigma}{t_j}\right)^3 \qquad S_4(\sigma) = t_j\left[-\left(\frac{\sigma}{t_j}\right)^2 + \left(\frac{\sigma}{t_j}\right)^3\right] \tag{4}$$

where $t_j = \frac{T}{M}$ is the time length of the j^{th} element, which is uniform across all the elements, and M is the total number of elements that discretize the time domain. Asymptotic convergence of the approximation to the exact solution is obtained by increasing the number of elements (Garg et al., 2006). The cubic Hermite polynomial trial functions used here satisfy the boundary displacement and velocity conditions. Substitution of the assumed solution to the delayed differential equations leads to a non-zero error. The errors can be weighted by a test functions, in which the integral of the weighted error is set to zero (Peters and Idzapanah, 1988). Here, the test functions are $\psi_1(\sigma) = 1$ and $\psi_2(\sigma) = \frac{\sigma}{t_j} - \frac{1}{2}$. On the j^{th} element, we have the following equations,

$$\int_0^{t_j}\left[\sum_{i=1}^{4} a_{ji}^n \ddot{S}_i\psi_p + 2\zeta\omega_n\sum_{i=1}^{4} a_{ji}^n \dot{S}_i\psi_p + \omega_n\sum_{i=1}^{4} a_{ji}^n S_i\psi_p\right]d\sigma -$$
$$\int_0^{t_j} Cb\left[f_0\psi_p - \sum_{i=1}^{4} a_{ji}^n S_i\psi_p + \sum_{i=1}^{4} a_{ji}^{n-1} S_i\psi_p\right]d\sigma = 0 \tag{5}$$

Here, $p = 1, 2$. This can be simplified in a compact matrix representation,

$$\begin{bmatrix} N_{11} & N_{12} & N_{13} & N_{14} \\ N_{21} & N_{22} & N_{23} & N_{24} \end{bmatrix}\begin{bmatrix} a_{j1} \\ a_{j2} \\ a_{j3} \\ a_{j4} \end{bmatrix}^n = \begin{bmatrix} C_1 \\ C_2 \end{bmatrix} + \begin{bmatrix} P_{11} & P_{12} & P_{13} & P_{14} \\ P_{21} & P_{22} & P_{23} & P_{24} \end{bmatrix}\begin{bmatrix} a_{j1} \\ a_{j2} \\ a_{j3} \\ a_{j4} \end{bmatrix}^{n-1} \tag{6}$$

where $N_{ip} = \int_0^{t_j}\left[\ddot{S}_i + 2\zeta\omega_n\dot{S}_i + \omega_n S_i\right]\psi_p d\sigma$, $C_p = \int_0^{t_j} Cbf_0\psi_p d\sigma$ and $P_{ip} = \int_0^{t_j} CbS_i\psi_p d\sigma$. For continuous cutting, the displacement and velocity at the end of j^{th} element are equal to that at the beginning of $(j+1)^{\text{th}}$ element, i.e., $\begin{bmatrix} a_{j1} \\ a_{j2} \end{bmatrix}^n = \begin{bmatrix} a_{(j-1)3} \\ a_{(j-1)4} \end{bmatrix}^n$. We can further derive a compact discrete dynamics form as $Na^n = Pa^{n-1} + Q$, and consequentially, $a^n = N^{-1}Pa^{n-1} + N^{-1}Q$. The asymptotic stability requires eigenvalues of $G = N^{-1}P$ within the unit circle of the complex plan, i.e., the maximum absolute eigenvalue is less than 1. In this study, we specified the physical parameters, including damping ratio ζ and natural frequency ω_n, for the experimental setup as determined from a detailed experimental modal analysis [13] and evaluated the stability over a range of process parameters (depth of cut, feed and spindle speed).

2.2 Real-time estimation of surface roughness

As mentioned in the foregoing, even under stable cutting conditions, anomalies leading to poor surface finish can still occur. A sensor-based model can be employed to predict surface roughness and anomalies in real-time using the vibration signal patterns. We collected *in situ* signals in the machining process with the experiment setup introduced in Section 2.

Surface defects such as mirror scratches and finish deterioration are attributed to the instability of system dynamics and therefore in-process monitored signals (e.g. cutting force and vibrations) that reflects process dynamics could be further employed to investigate the relationship between surface characteristics and UPM dynamics (He et al., 2007). Consequently, extracted features from those collected raw signals could be used as effective measures that quantify the surface characteristics.

We extracted time domain statistical features from the raw signals, including absolute mean, standard deviation, skewness, kurtosis and root mean square. But those features are not sufficient to capture the nonlinear dynamics of UPM process. Notably, recent development of nonlinear dynamics has provided alternative options for nonlinear time series analysis and feature extraction. One of the most important methods is recurrence quantification analysis (RQA). A recurrence plot (see Figure 4)

provides a global picture of the autocorrelation in a time series over the time domain. According to Taken's theorem (Takens, 1981), the system dynamics can be adequately reconstructed by the individual measurement, using the time-delay coordinate. With time delay τ and embedded dimension d, state space vector $s(i) = [x(i) - (d-1)\tau, x(i) - (d-2)\tau, \dots, x(i)]$ can be reconstructed using the feed vibration signals from UPM. Recurrence plot (RP) can capture the topological relationships existing in the reconstructed state space. The RQA is based on the threshold recurrence plot (TRP), which is expressed by the recurrence matrix

$$\boldsymbol{R}(i,j) = \Theta(\epsilon - \| s(i) - s(j) \|) \qquad i,j = 1,2,\dots,n \tag{7}$$

Here, n is the total number of state space vectors, ε is the cutoff distance or threshold, Θ is the Heaviside function ($\Theta(x) = 0$ if $x < 0$ and $\Theta(x) = 1$ otherwise), and $\|\cdot\|$ is a norm (Marwan et al., 2007). The pixel in RP plane lying at (i,j) is black if $R(i,j) = 1$ and white if $R(i,j) = 0$. Hence, a recurrence plot shows the time at which a state of the dynamical system exhibits recurrence. Here we use small recurrence rate within the range of 0.1%-5.0% (Webber Jr and Zbilut, 1994). The embedded state space plot for the vibration signal in the vertical direction was shown in Figure 4 (a) with time delay τ obtained by mutual information (Fraser and Swinney, 1986) and embedded dimension d got by False Nearest Neighborhood (Kennel et al., 1992). Distances among the state space vectors were presented in the RP in Figure 4 (b), with the dark dot representing the distance that is less than the threshold ϵ. Clearly, there are some distinct topology and texture patterns of the RP; for instance, some of the dark dots form lines paralleling to the main diagonal line. In order to quantitatively characterize the RP patterns, RQA was extracted, which has greater sensitivity to the changing dynamics, making these ideal candidates for features.

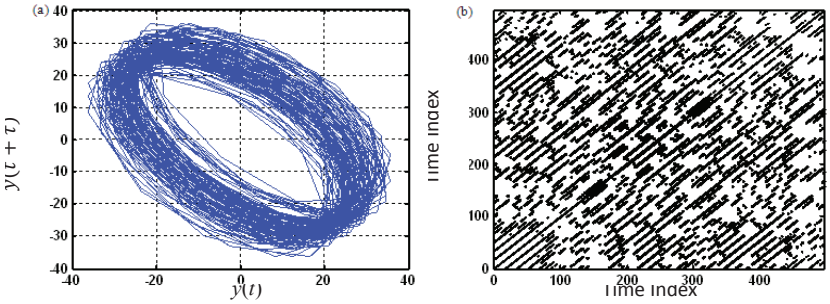

Figure 4: (a) Reconstructed vibration signal in state space and (b) threshold recurrence plot of the vibration signal in Y-axis (vertical direction)

In this study, we extracted 5 statistical features and 7 RQA features (namely, recurrence rate, determinism, maximum length, trend, laminarity, trapping time and entropy (Marwan et al., 2007)) for each signal. Altogether, we have 72 features extracted from the 6 signals (vibration and force signals from X,Y and Z axes). As UPM signals contain significant amount of redundant information (Rao et al., 2014), and some features can be highly correlated. Principal component analysis (PCA) was employed to get the uncorrelated principal components from the original redundant features, which along with the process parameters for each marked sample zone (feed, depth of cut and cutting speed) were considered as the key process input variable (KPIV) to estimate Ra for 16 zones on the workpiece (each zone forms 4.5 mm wide ring). Nonparametric Gaussian process (GP) regression model was used here for Ra estimation (Rasmussen and Williams, 2006). Compared with other estimation methods, Gaussian process regression model can not only provide a point estimate, but a complete distribution of Ra since it generates posterior distribution of predicted Ra value.

3 Experimental verification, results and discussion

In this section, the process stability investigation using direct simulation model and TFEM approximation are presented, and the surface roughness Ra estimation based on sensor signal features is also discussed.

3.1 Stability analysis using model simulation

The simulation of the original model was used to explore UPM process dynamics at different parameter settings. Figure 5 shows the simulated vibration signals as we increased the depth of cut from 0.2 μm to 10 μm, with the feed and spindle speed fixed at 6 μm/min and 500 RPM. At depth of cut of 0.2 μm, the vibration amplitude tends to decrease because of the system damping, resulting in a point attractor or equilibrium focus (see Figure 5 (a)); the dynamics rests at a constant vibration level at depth of cut of 5.17 μm as well as 7 μm, leading to periodic attractor (see Figure 5 (b) and (c)). Further study showed that the periodic attractor of dynamics happens at depth of cut around 5 μm, which is consistent with the TFEM study indicated in Section 3.2.

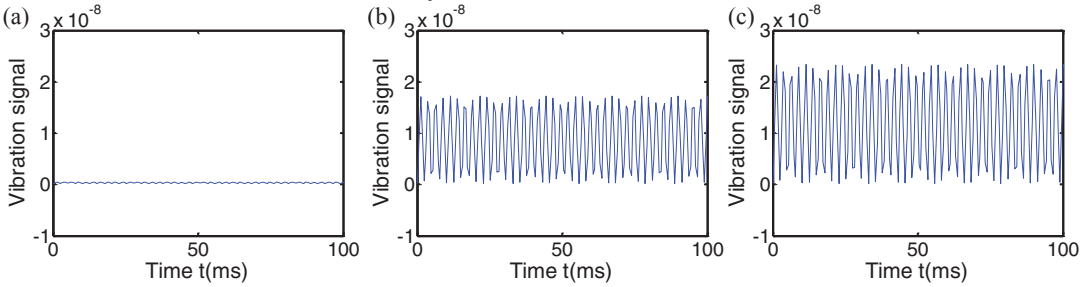

Figure 5: Vibration signal from simulations at depth cut of (a) 0.2 μm, (b) 5.17 μm and (c) 7 μm

Recurrence Measure	From experiment	From simulation
Recurrence Rate	0.2787	0.3060
Laminarity	0.5695	0.4772
Trapping Time	2.5821	2.0000
Recurrence time of 1st type	3.5129	3.2739
Recurrence time of 2nd type	5.4214	4.3183
Recurrence period density entropy	0.4771	0.2369

Table 1: Comparison of RQA for experimental records and simulation with process parameters feed 6 μm/min, spindle speed 500 RPM and depth of cut 5 μm

To validate the simulation model, we compared the RQA of the vibration signals from simulation and experiment. As summarized in Table 1, most differences are less than 30%, indicating the effectiveness of the simulation to capture the nonlinear dynamics of UPM process.

3.2 Stability analysis using TFEM approximation and experimental verification

As noted in the foregoing, the model is not tractable for developing stability lobes. Therefore we implemented the TFEM with a simplified model under different process conditions, namely, feed rate, depth of cut and spindle speed to obtain stability lobes. As shown in Figure 6, the area below the dark patch has eigenvalues less than 0.9, and area above the gray patch larger than 1.1. As uncertainty arises during practical machining operations, which is attributed to measurement error (e.g., tool radius and stiffness estimation) or flow stress modeling/estimation, one may observe that the stability of the actual process does not match the stability lobe from TFEM simulations exactly. Recently,

Ahmadi and Ismail (Ahmadi and Ismail, 2010) associated the stability lobes with different vibration amplitudes. In contrast to the single boundary between "highly stable" (vibration dies down to zero amplitude) and "fully unstable" (vibration amplitude stabilizes at an arbitrarily large value), they defined an intermediate state of "finite amplitude stability", where the amplitude of vibrations stabilizes between zero and the certain value. Theoretical and experimental studies also suggested instead of a single boundary, a band exists between stable and unstable regions (Ahmadi and Ismail, 2010). Hence, a stability band provided in Figure 6 can be much helpful while simplifying nonlinear models akin to UPM process.

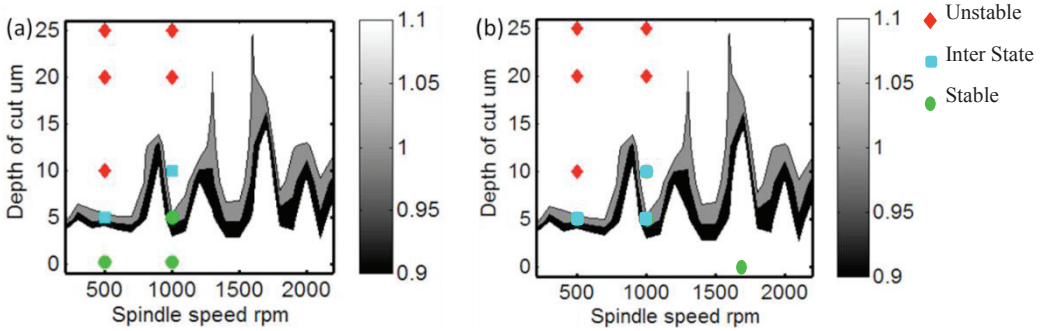

Figure 6: Stability lobe diagram from TFEM model at feed = 6 μm/min and comparison with (a) direct simulation (green/round: stable state, cyan/square: intermediate state, red/diamond: unstable) and (b) experiment records

To validate the TFEM model, we consider Ra values as criterion determining the stability under each machining condition and compared the stability diagram obtained from TFEM with direct simulation and our experimental records. The comparison with direct simulation is shown in Figure 6(a), with the round shape representing unstable dynamics, square shape the intermediate state and diamond the unstable cutting. Note that in the TFEM model, we linearized the thrust force expression around the nominal feed f_0, therefore there is slight difference between TFEM and direct simulation, and the stability band can be used to capture the difference. Given feed at 6 μm/min, by examining the distribution of Ra values, we concluded that Ra>90 nm can represent instability, and Ra below 90 nm indicates stable machining conditions (see Figure 6(b), where green round shape represents stable conditions, and red diamond represents unstable conditions). Overall, at least 70% of validation points agree with the TFEM models. Note that, the periodic attractor at 500 RPM is also consistent with the stability band indicated in the stability lobe diagram. This implies that in UPM a single boundary may not represent the true dynamics, and the band occurs at the process parameters that lead to periodic attractor.

3.3 Surface roughness estimation

Recent advances in wireless sensors, communication and computing technologies, as well as the availability of cloud computing and big data have made sensor-based analytical models applicable for real-time quality control in complex ultra-precision manufacturing processes. However, the nonlinear and nonstationary nature of the machining signals has largely limit the applicability of conventional sensor-based modeling techniques (Cheng et al., Accepted). Our physical model here can identify the stable cutting conditions, and the signals collected at stable dynamics enable us to accurately capture Ra variation.

The dataset was randomly divided into training part and testing part. The model was run multiple times to test the robustness of GP method for surface roughness prediction. The input is the process parameters (depth of cut, feed and cutting speed) and the first 4 principal components. Figure 7 (a) illustrates the estimation result for 80 sample points. The gray region represents the 2-sigma interval.

As we can see, most of the observation values of Ra lay in this interval. The comparison of the observation value and estimation value of Ra was shown in Figure 7 (b), indicating the high correlation between the observed and estimated Ra values. The model can predict the surface roughness with small residual for most sample points.

Table 2 summarizes the performance of Gaussian process regression model. The mean R^2 obtained was 0.83, which indicates the goodness-of-fit of the Gaussian process regression model. In addition, based on the hyperparameters of GP model, we conclude that cutting speed is not so important towards determining the surface roughness over the cutting condition studied.

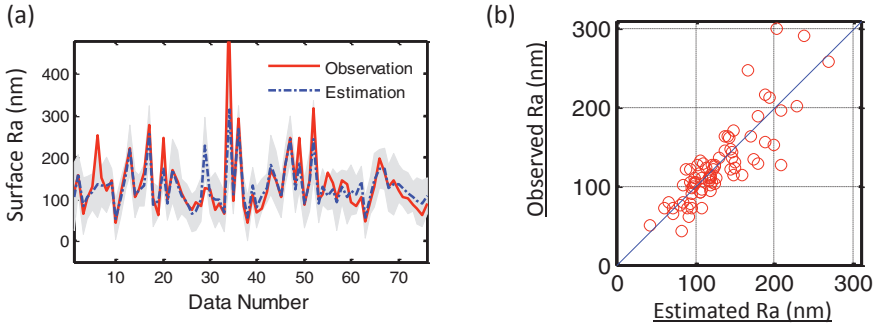

Figure 7: (a) Ra estimation result with 2-sigma interval by GP model; (b) comparison of the measured Ra vs. Ra value estimated by GP model

	Mean	Standard deviation
R^2	0.83	0.11
RMS	21.4	4.37

Table 2: Ra prediction accuracy using measures as R^2 and root-mean-square

4 Conclusions

UPM has been widely used in industry for various critical product applications to achieve surface roughness within the range of 1-10nm. Detection of surface variations is crucial for UPM quality control, which is heavily dependent on the process dynamics. The research to address real-time surface variation monitoring in UPM can be summarized as follows:

1. A physical model was developed to allow the simulation of UPM process dynamics by considering the combined round tool edge and ploughing effects in UPM. The direct simulation of DDE indicated 3 different dynamic behaviors, namely, equilibrium focus, periodic attractor, and unsteady behavior. The dynamic regimes are validated against our experiment recordings.
2. We investigated TFEM approximation of the DDE for faster stability identification with simplified force representation. Experimental investigations suggest that the model predictions of stability characteristics match 70% of the experimental observations.
3. Sensor fusion technique was employed for real-time surface roughness estimation. With the features extracted from vibration and force signals, Gaussian process regression model registered surface roughness (Ra) estimation accuracy over 0.8, suggesting the effectiveness of real-time Ra estimation.

These investigations suggest that the combination of the physical dynamics and sensor-based data-driven models enables us to choose suitable “stable” process conditions to yield surface finish

Ra in 10-50 nm range, and estimate the surface roughness changes in real-time.

Acknowledgements

The authors would like to acknowledge the support of the National Science Foundation (Grants No. CMMI-1432914 and CMMI-1437139) and Rockwell international professorship.

References

AHMADI, K. & ISMAIL, F. 2010. Machining chatter in flank milling. *International Journal of Machine Tools and Manufacture,* 50**,** 75-85.

ALTINTAS, Y., EYNIAN, M. & ONOZUKA, H. 2008. Identification of dynamic cutting force coefficients and chatter stability with process damping. *CIRP Annals - Manufacturing Technology,* 57**,** 371-374.

ALTINTAS, Y. & WECK, M. 2004. Chatter stability of metal cutting and grinding. *CIRP Annals - Manufacturing Technology,* 53**,** 619-642.

BAYLY, P. V., HALLEY, J. E., MANN, B. P. & DAVIES, M. A. 2003. Stability of interrupted cutting by temporal finite element analysis. *Journal of Manufacturing Science and Engineering,* 125**,** 220-225.

CHAE, J., PARK, S. S. & FREIHEIT, T. 2006. Investigation of micro-cutting operations. *International Journal of Machine Tools and Manufacture,* 46**,** 313-332.

CHENG, C., SA-NGASOONGSONG, A., BEYCA, O., LE, T., YANG, H., KONG, Z. & BUKKAPATNAM, S. T. S. Accepted. Time series forecasting for nonlinear and nonstationary processes: a review and comparative study. *IIE Transactions*.

DE BARROS, M. I., VANDENBULCKE, L. & BLÉCHET, J. J. 2001. Influence of diamond characteristics on the tribological behaviour of metals against diamond-coated Ti–6Al–4V alloy. *Wear,* 249**,** 67-77.

DORNFELD, D., MIN, S. & TAKEUCHI, Y. 2006. Recent advances in mechanical micromachining. *CIRP Annals - Manufacturing Technology,* 55**,** 745-768.

FRASER, A. M. & SWINNEY, H. L. 1986. Independent coordinates for strange attractors from mutual information. *Physical Review A,* 33**,** 1134.

GARG, N. K., MANN, B. P., KIM, N. H. & KURDI, M. H. 2006. Stability of a time-delayed system with parametric excitation. *Journal of Dynamic Systems, Measurement, and Control,* 129**,** 125-135.

HE, Q., KONG, F. & YAN, R. 2007. Subspace-based gearbox condition monitoring by kernel principal component analysis. *Mechanical Systems and Signal Processing,* 21**,** 1755-1772.

IKAWA, N., DONALDSON, R. R., KOMANDURI, R., KÖNIG, W., AACHEN, T. H., MCKEOWN, P. A., MORIWAKI, T. & STOWERS, I. F. 1991. Ultraprecision Metal Cutting — The Past, the Present and the Future. *CIRP Annals - Manufacturing Technology,* 40**,** 587-594.

JIN, X. & ALTINTAS, Y. 2013. Chatter stability model of micro-milling with process damping. *Journal of Manufacturing Science and Engineering,* 135**,** 031011-031011.

KENNEL, M. B., BROWN, R. & ABARBANEL, H. D. I. 1992. Determining embedding dimension for phase-space reconstruction using a geometrical construction. *Physical Review A,* 45**,** 3403.

KOMANDURI, R., CHANDRASEKARAN, N. & RAFF, L. M. 2000. M.D. Simulation of nanometric cutting of single crystal aluminum-effect of crystal orientation and direction of cutting. *Wear,* 242**,** 60-88.

LEE, W. B., CHEUNG, C. F. & TO, S. 1999. Materials induced vibration in ultra-precision machining. *Journal of Materials Processing Technology,* 89-90**,** 318-325.

LIU, K., LI, X. P. & LIANG, S. Y. 2001. Modeling of ductile cutting of tungsten carbide. *Transactions*

of the North American Manufacturing Research Institution of SME, 29**,** 251-258.
LIU, X., DEVOR, R. E., KAPOOR, S. G. & EHMANN, K. F. 2004. The mechanics of machining at the microscale: assessment of the current state of the science. *Journal of Manufacturing Science and Engineering,* 126**,** 666-678.
MARWAN, N., CARMEN ROMANO, M., THIEL, M. & KURTHS, J. 2007. Recurrence plots for the analysis of complex systems. *Physics Reports,* 438**,** 237-329.
PATRIKAR, R. M. 2004. Modeling and simulation of surface roughness. *Applied Surface Science,* 228**,** 213-220.
PETERS, D. A. & IDZAPANAH, A. P. 1988. hp-Version Finite Elements for the Space-Time Domain. *Computational Mechanics,* 3**,** 73-88.
RAO, P., BUKKAPATNAM, S., BEYCA, O., KONG, Z. & KOMANDURI, R. 2014. Real-Time Identification of Incipient Surface Morphology Variations in Ultraprecision Machining Process. *Journal of Manufacturing Science and Engineering,* 136**,** 021008-021008.
RASMUSSEN, C. E. & WILLIAMS, C. K. I. 2006. *Gaussian Prcoess for Machine Learning,* Cambridge, MA, MIT Press.
SON, S. M., LIM, H. S. & AHN, J. H. 2005. Effects of the friction coefficient on the minimum cutting thickness in micro cutting. *International Journal of Machine Tools and Manufacture,* 45**,** 529-535.
STEPAN, G., SZALAI, R., MANN, B. P., BAYLY, P. V., INSPERGER, T., GRADISEK, J. & GOVEKAR, E. 2004. Nonlinear Dynamics of High-Speed Milling—Analyses, Numerics, and Experiments. *Journal of Vibration and Acoustics,* 127**,** 197-203.
TAKENS, F. 1981. Detecting strange attractors in turbulence. *Lecture Notes in Mathematics.* Springer, Berlin.
VENKATACHALAM, S. & LIANG, S. Y. 2006. Effects of ploughing forces and friction coefficient in microscale machining. *Journal of Manufacturing Science and Engineering,* 129**,** 274-280.
WALDORF, D. J., DEVOR, R. E. & KAPOOR, S. G. 1999. An evaluation of ploughing models for orthogonal machining. *Journal of Manufacturing Science and Engineering,* 121**,** 550-558.
WEBBER JR, C. L. & ZBILUT, J. P. 1994. Dynamical assessment of physiological systems and states using recurrence plot strategies. *Journal of Applied Physiology,* 76**,** 965-973.